AIP Applied Physics Letters

CdSe/CdTe type-II superlattices grown on GaSb (001) substrates by molecular beam epitaxy

Jing-Jing Li, Xinyu Liu, Shi Liu, Shumin Wang, David J. Smith, Ding Ding, Shane R. Johnson, Jacek K. Furdyna, and Yong-Hang Zhang

Citation: Applied Physics Letters **100**, 121908 (2012); doi: 10.1063/1.3697676
View online: http://dx.doi.org/10.1063/1.3697676
View Table of Contents: http://scitation.aip.org/content/aip/journal/apl/100/12?ver=pdfcov
Published by the AIP Publishing

Articles you may be interested in

Optimization of growth conditions of type-II Zn(Cd)Te/ZnCdSe submonolayer quantum dot superlattices for intermediate band solar cells
J. Vac. Sci. Technol. B **31**, 03C119 (2013); 10.1116/1.4797486

Photoluminescence studies of type-II CdSe/CdTe superlattices
Appl. Phys. Lett. **101**, 061915 (2012); 10.1063/1.4745199

Structural properties and spatial ordering in multilayered ZnMgTe/ZnSe type-II quantum dot structures
J. Appl. Phys. **111**, 033516 (2012); 10.1063/1.3681812

Quality improvements of Zn x Cd y Mg 1−x−y Se layers grown on InP substrates by a thin ZnCdSe interfacial layer
Appl. Phys. Lett. **72**, 1317 (1998); 10.1063/1.120980

In situ photoemission and reflectance anisotropy spectroscopy studies of CdS grown on InP(001)
J. Vac. Sci. Technol. B **15**, 1260 (1997); 10.1116/1.589447

This article is copyrighted as indicated in the article. Reuse of AIP content is subject to the terms at: http://scitation.aip.org/termsconditions. Downloaded to IP: 209.147.144.22 On: Wed, 04 Feb 2015 17:39:22

APPLIED PHYSICS LETTERS **100**, 121908 (2012)

CdSe/CdTe type-II superlattices grown on GaSb (001) substrates by molecular beam epitaxy

Jing-Jing Li,[1,2] Xinyu Liu,[3] Shi Liu,[1,2] Shumin Wang,[1,2] David J. Smith,[1,4] Ding Ding,[1,2] Shane R. Johnson,[1,2] Jacek K. Furdyna,[3] and Yong-Hang Zhang[1,2,a)]
[1]*Center for Photonics Innovation, Arizona State University, Tempe, Arizona 85287, USA*
[2]*School of Electrical, Computer and Energy Engineering, Arizona State University, Tempe, Arizona 85287, USA*
[3]*Department of Physics, University of Notre Dame, Notre Dame, Indiana 46556, USA*
[4]*Department of Physics, Arizona State University, Tempe, Arizona 85287, USA*

(Received 21 February 2012; accepted 5 March 2012; published online 22 March 2012)

CdSe/CdTe superlattices are grown on GaSb substrates using molecular beam epitaxy. X-ray diffraction measurements and cross-sectional transmission electron microscopy images indicate high crystalline quality. Photoluminescence (PL) measurements show the effective bandgap varies with the superlattice layer thicknesses and confirm the CdSe/CdTe heterostructure has a type-II band edge alignment. The valence band offset between unstrained CdTe and CdSe is determined as 0.63 ± 0.06 eV by fitting the measured PL peak positions using the envelope function approximation and the Kronig-Penney model. These results suggest that CdSe/CdTe superlattices are promising candidates for multi-junction solar cells and other optoelectronic devices based on GaSb substrates. © *2012 American Institute of Physics*. [http://dx.doi.org/10.1063/1.3697676]

Monolithic integration of II-VI (MgZnCd)(SeTe) and III-V (AlGaIn)(AsSb) semiconductors on commercially available GaSb or InAs substrates has been proposed as a platform for many electronic and optoelectronic devices.[1–4] These two families of semiconductor materials have identical crystalline structures and very similar thermal expansion coefficients, and they can be grown lattice-matched on GaSb or InAs substrates with low defect densities. Furthermore, these materials are ideal for multi-junction solar cells, as their direct bandgaps allow the use of thin absorbing layers that can be current-matched to efficiently capture the entire solar spectrum. Several multi-junction solar cell structures have been designed with the potential to reach ultra-high conversion efficiency.[1,4]

In the proposed solar cell designs, a zinc blende CdSeTe alloy lattice matched to the GaSb substrates is used as one of the subcells. However, there have been only a few successful attempts reported at growing zinc-blende CdSeTe random alloys on Si substrates, and it is difficult to achieve large Se compositions because of the high vapor pressure of group VI elements and the low sticking probability of Se atoms.[5–8] In the current work, CdSe/CdTe superlattices are proposed as an alternative to the random CdSeTe alloys, and a series of these superlattice structures are grown on GaSb (001) substrates using molecular beam epitaxy (MBE). While the ZnSe/ZnTe system has been intensively investigated,[9,10] little work has so far been done for the CdSe/CdTe system.[11–13] In particular, there was no experimental papers reporting the properties of CdSe/CdTe superlattices or the valence band offset between CdSe and CdTe. In order to address these issues, this work reports the growth and the structural and optical characterization of a series of CdSe/CdTe superlattices.

The epitaxial growth of the superlattice samples was carried out using a dual-chamber Riber 32P MBE system consisting of III-V and II-VI chambers connected by an ultra high-vacuum transfer module. The structures were grown on undoped epi-ready GaSb (001) substrates. First, the substrate oxide was thermally removed by heating up to 510 °C under an antimony flux in the III-V chamber, while the process was monitored using reflection high-energy electron diffraction (RHEED). Next, a 100 nm GaSb buffer layer was grown at 470 °C. The substrate was then transferred to the II-VI chamber, where a ZnTe buffer layer was grown at 320 °C under a Zn flux initiated prior to the growth.[2] The CdSe/CdTe superlattice was then grown at 320 °C using the modulation of Te and Se shutters while keeping the Cd shutter open. During the growth, the beam equivalent pressure (BEP) ratio of Te/Cd and Se/Cd were kept at 2:1 and 4:1, respectively.

Three CdSe/CdTe superlattice structures (labeled A, B, and C) were grown with the various layer thicknesses shown in Table I and are expected to have different effective bandgap energies. During the growth of sample B, the Cd shutter remained open for 5 s while all the other shutters were closed after the growth of the CdSe layer, in order to reduce the intermixing of Se and Te at the CdSe/CdTe interface. The RHEED patterns of samples A and C changed from streaky to spotty during the growth, suggesting a 3D growth mode at the end of the growth. In contrast, the RHEED pattern of sample B remained streaky through to the end, which suggests that this sample has better crystalline quality and layer uniformity than the other two samples. Note that all the CdSe/CdTe superlattices have the same zinc blende structure as the substrate, as shown by the RHEED patterns and confirmed by the x-ray diffraction (XRD) and transmission electron microscopy (TEM) observations.

High-resolution XRD measurements of the samples were performed for the symmetric (004) and asymmetric (113) reflections using the Cu Kα_1 radiation on a PANalytical X'Pert PRO Materials Research Diffractometer. Figures 1(a)–1(c) show the (004) ω-2θ diffraction patterns of

a)Electronic mail: yhzhang@asu.edu.

This article is copyrighted as indicated in the article. Reuse of AIP content is subject to the terms at: http://scitation.aip.org/termsconditions. Downloaded to IP: 209.147.144.22 On: Wed, 04 Feb 2015 17:39:22

TABLE I. Structures and optical transition energies of the studied samples.

Sample	$a_{//}$ (Å)	$a_{\perp}$ (Å)	Thickness (nm)		PL peak position at 10 K (eV)	Calculated Eg at 0 K (eV)
			CdSe	CdTe		
A	6.103	6.101	10.52	1.51	1.04	1.05
B	6.097	6.120	5.47	0.88	1.18	1.22
C	6.096	6.096	5.99	0.75	1.30	1.26

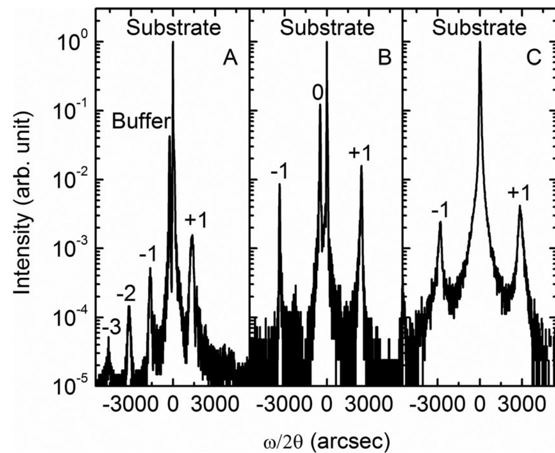

FIG. 1. X-ray (004) $\omega/2\theta$ diffraction patterns of samples A (a), B (b), and C (c).

samples A, B, and C, which respectively consists of 40, 40, and 50 periods of CdTe and CdSe layers. The lattice constants of GaSb and ZnTe are 6.096 and 6.105 Å, respectively, and the lattice constants of CdSe and CdTe are 6.052 and 6.482 Å, respectively. Therefore, the CdTe layer is compressively strained to the GaSb substrate or the ZnTe buffer layer, while the CdSe layer is tensilely strained. The high structural qualities of the samples are evidenced by the sharp satellite peaks and the absence of appreciable peak broadening. The lateral and average vertical lattice constants $a_{//}$ and $a_{\perp}$ of the superlattices shown in Table I are determined from the zeroth superlattice peaks in the (004) and (113) XRD patterns, and the layer thicknesses are determined from the separation of the first-order superlattice peaks in the (004) XRD patterns. Sample A has a ZnTe buffer layer of approximately 200 nm, and the superlattice is strained as shown by its lateral and vertical lattice constants. The ZnTe buffer layers of samples B and C are about 10 nm thick, and the superlattice of sample B is strained while that of sample C is almost perfectly lattice matched to the substrate. It can also be seen in Fig. 1 that the superlattice peaks of sample B have the narrowest FWHM, indicating that this sample has minimal interface roughness as well as the fewest defects.

Specimens of sample B suitable for cross-sectional TEM observation were prepared by standard mechanical polishing, dimpling, and a final argon-ion-milling at reduced energy (2-2.5 keV), with the sample being held at liquid-nitrogen temperature to minimize artifacts due to thermal or ion-beam damage during milling. The low magnification image shown in Fig. 2(a) demonstrates the overall high structural-quality and regularity of the CdSe/CdTe superlattice. In addition, the satellite diffraction spot adjacent to the major diffraction spot visible in selected area electron diffraction pattern, as shown in the inset of Fig. 2(a), confirms the uniformity of the layer thicknesses. The high-resolution lattice image of this same specimen shown in Fig. 2(b)

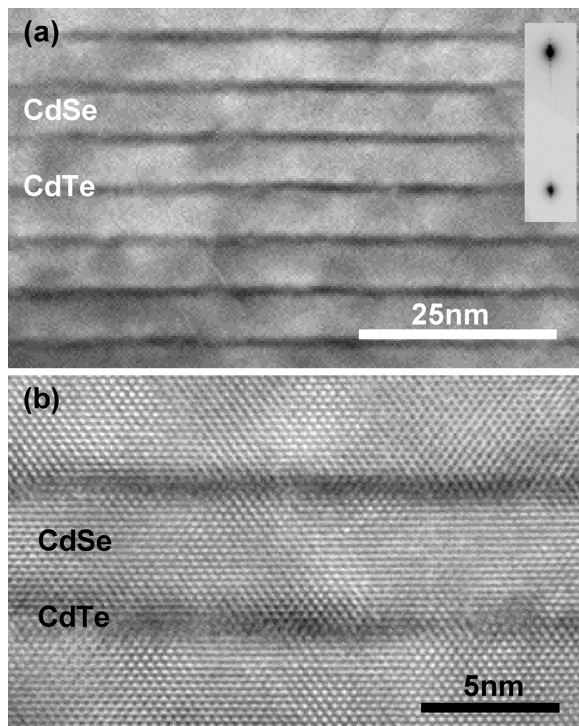

FIG. 2. Structural characterization of sample B using TEM. (a) Cross-sectional image showing regular superlattice periodicity and the absence of major structural defects, as confirmed by the selected area electron diffraction pattern shown in the inset. (b) High-resolution lattice image showing excellent crystallinity.

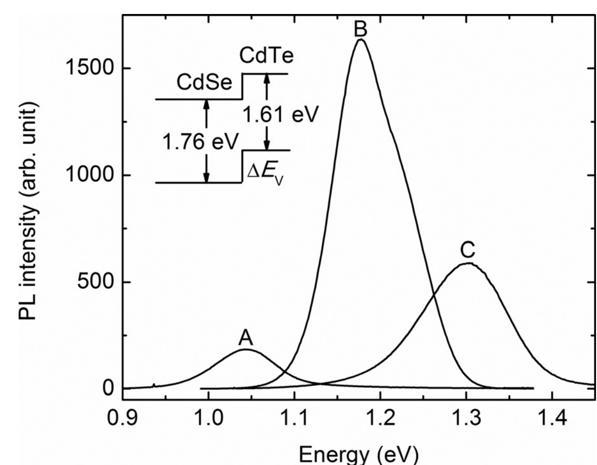

FIG. 3. Photoluminescence spectra of samples A, B, and C measured at 10 K. The difference in the PL peak positions is a result of the different layer thicknesses in each superlattice.

This article is copyrighted as indicated in the article. Reuse of AIP content is subject to the terms at: http://scitation.aip.org/termsconditions. Downloaded to IP: 209.147.144.22 On: Wed, 04 Feb 2015 17:39:22

TABLE II. Material parameters of CdSe and CdTe used in the Kronig-Penney model.

	a (Å)	Eg (eV)	m_e	m^z_{hh}	m^z_{lh}	a_c (eV)[25]
CdSe	6.052 (Ref. 12)	1.76 (Refs. 12 and 20)	0.12 (Ref. 15)	0.83 (Ref. 19)	0.13 (Ref. 19)	−3.77
CdTe	6.482 (Refs. 12 and 24)	1.61 (Refs. 12, 16, and 24)	0.088 (Ref. 17)	0.53 (Refs. 17 and 18)	0.11 (Refs. 17 and 18)	−5.09

	a_v (eV)[25]	b (eV)[23]	C_{11} (10^{11} dyne/cm^2)	C_{12} (10^{11} dyne/cm^2)
CdSe	−1.81	−0.8	8.8 (Ref. 22)	5.3 (Ref. 22)
CdTe	−2.14	−1	5.35 (Refs. 21 and 24)	3.68 (Refs. 21 and 24)

demonstrates very-high crystalline-quality at the atomic length scale.

It has been reported that the unstrained CdTe and CdSe forms a type-II band edge alignment[11,12] with the respective bandgap energies 1.76 eV (Refs. 12 and 20) and 1.61 eV (Refs. 12, 16, and 24) at 10 K. In the superlattice structures studied here, the band edges are modified by a combination of the hydrostatic and shear strains. The hydrostatic strain shifts the conduction band and valence band edges, while the shear strain splits the heavy hole and light hole bands. The superlattice minibands are formed as the hybridization of the bound states in the quantum wells coupled through the barriers.

To study the impact of band alignment on the proposed superlattice materials, photoluminescence (PL) measurements of samples A, B, and C were performed using a 660-nm diode laser with an excitation power density of 180 W/cm^2. Photoluminescence is observed at both room temperature and low temperature. The 10 K measurement results plotted in Fig. 3 show that the PL spectra of the three samples peak at different wavelengths due to the different superlattice period of each sample. The ground state transition energy of sample B shows the strongest PL intensity and the narrowest FWHM. Furthermore, due to the type-II band edge alignment between CdTe and CdSe (see Fig. 3 inset), the PL peak energies are considerably lower than the bandgap energy of either CdTe or CdSe.

The conduction and valence band ground state energy levels of the three samples were calculated using the Kronig-Penney model,[14] with the layer thicknesses given in Table I, the material parameters shown in Table II, and the valence band offset ΔE_V as a fitting parameter. The valence band offset ΔE_V determined by fitting the calculated ground state transition energies to the measured PL peak positions is 0.63 ± 0.06 eV, which agrees with the theoretical prediction of 0.57 eV (Ref. 12) within the experimental error. The calculated ground state transition energies of the samples are in reasonable agreement with the measured PL peak positions as shown in Table I.

In conclusion, a series of CdSe/CdTe superlattices with different layer thicknesses are grown on GaSb substrates by MBE. The superlattices exhibit high structural quality as shown by the sharp satellite peaks in high-resolution XRD patterns, smooth interfaces in high-resolution TEM micrographs, and clear electron diffraction patterns. PL measurements show that the ground state transition energies of the superlattices are smaller than the bandgap of either constituent material and hence establish the existence of a strong type-II band alignment. The type-II valence band offset between unstrained CdSe and CdTe is determined as 0.63 ± 0.06 eV by fitting the PL peak positions of superlattices with different layer thicknesses to the ground state transition energies calculated using the Kronig-Penney model.

This work is partially supported by the Science Foundation Arizona, Contract No. SRG 0339-08, the Air Force Research Laboratory/Space Vehicles Directorate, Contract No. FA9453-08-2-0228, and by NSF grant ECCS-1002072. Jing-Jing Li would like to thank Jin Fan for discussion of XRD data analysis.

[1]Y.-H. Zhang, S.-N. Wu, D. Ding, S.-Q. Yu, and S. R. Johnson, in Proceedings of the 33th IEEE Photovoltaics Specialist Conference, San Diego, California, May 11–16, 2008, p. 1–5.
[2]S. Wang, D. Ding, X. Liu, X.-B. Zhang, D. J. Smith, J. K. Furdyna, and Y.-H. Zhang, J. Cryst. Growth **311**, 2116 (2009).
[3]J. Fan, L. Ouyang, X. Liu, D. Ding, J. K. Furdyna, D. J. Smith, and Y.-H. Zhang, J. Cryst. Growth **323**, 127 (2011).
[4]S.-N. Wu, D. Ding, S. R. Johnson, S.-Q. Yu, and Y.-H. Zhang, Prog. Photovoltaics **18**, 328 (2010).
[5]N. Matsumura, T. Sakamoto, and J. Saraie, J. Cryst. Growth **251**, 602 (2003).
[6]Y. P. Chen, G. Brill, and N. K. Dhar, J. Cryst. Growth **252**, 270 (2003).
[7]G. Brill, Y. Chen, P. M. Amirtharaj, W. Sarney, D. Chandler-Horowitz, and N. K. Dhar, J. Electron. Mater. **34**, 655 (2005).
[8]F. Z. Amira, K. Clarka, E. Maldonadoa, W. P. Kirka, J. C. Jiangb, J. W. Ager, III, K. M. Yu, and W. Walukiewicz, J. Cryst. Growth **310**, 1081 (2008).
[9]I. L. Kuskovsky, C. Tian, G. F. Neumark, J. E. Spanier, I. P. Herman, W.-C. Lin, S. P. Guo, and M. C. Tamargo, Phys. Rev. B **63**, 155205 (2001).
[10]Y. Gu, I. L. Kuskovsky, M. van der Voort, G. F. Neumark, X. Zhou, and M. C. Tamargo, Phys. Rev. B **71**, 045340 (2005).
[11]C. H. Wang, T. T. Chen, K. W. Tan, Y. F. Chen, C. T. Cheng, and P. T. Chou, J. Appl. Phys. **99**, 123521 (2006).
[12]S.-H. Wei, S. B. Zhang, and A. Zunger, J. Appl. Phys. **87**, 1304 (2000).
[13]X. Zhang, S. Wang, D. Ding, X. Liu, J.-H. Tan, J. K. Furdyna, Y.-H. Zhang, and D. J. Smith, J. Electron. Mater. **38**, 1558 (2009).
[14]S. L. Chuang, *Physics of Optoelectronic Devices* (Wiley, New York, 1995).
[15]Y. D. Kim, M. V. Klein, S. F. Ren, Y. C. Chang, H. Luo, N. Samarth, and J. K. Furdyna, Phys. Rev. B **49**, 7262 (1994).
[16]J. Camassel and D. Auvergne, Phys. Rev. B **12**, 3258 (1975).
[17]L. S. Dang, G. Neu, and R. Romestain, Solid State Commun. **44**, 1187 (1982).
[18]P. Lawaetz, Phys. Rev. B **4**, 3460 (1971).
[19]M. Willatzen, M. Cardona, and N. Christensen, Phys. Rev. B **51**, 17992 (1995).
[20]W. Shan, J. Song, H. Luo, and J. Furdyna, Phys. Rev. B **50**, 8012 (1994).
[21]H. J. McSkimin and D. G. Thomas, J. Appl. Phys. **33**, 56 (1962).
[22]E. Deligoz, K. Colakoglu, and Y. Ciftci, Physica B **373**, 124 (2006).
[23]S. Adachi, *Properties of Group-IV, III-V and II-VI Semiconductors* (Wiley, Chichester, 2005).
[24]A. J. Strauss, Rev. Phys. Appl. **12**, 167 (1977).
[25]S.-H. Wei and A. Zunger, Phys. Rev. B **60**, 5404 (1999).

This article is copyrighted as indicated in the article. Reuse of AIP content is subject to the terms at: http://scitation.aip.org/termsconditions. Downloaded to IP: 209.147.144.22 On: Wed, 04 Feb 2015 17:39:22